ISX promotes tumor migration and invasion in lung cancer by upregulating COL1A1 *in vitro*

YIHE MA[1,2*], YE CHEN[3*], YUHUI LIANG[2*], YUN HUANG[1], MIAO GONG[1], LIFENG TIAN[1], XIAOJUN XIAO[2,4], JINGYAN LIU[5] and QINMIAO HUANG[1]

[1]Department of Respiratory Medicine and Allergy, The Third Affiliated Hospital (The Affiliated Luohu Hospital) of Shenzhen University, Shenzhen, Guangdong 518000, P.R. China; [2]Shenzhen Key Laboratory of Allergy and Immunology, State Key Laboratory of Respiratory Disease Shenzhen University Division, Shenzhen University Medical School, Shenzhen University, Shenzhen, Guangdong 518000, P.R. China; [3]Department of Pediatric Medicine, Shenzhen Nanshan People's Hospital, Shenzhen, Guangdong 518000, P.R. China; [4]Guangdong Provincial Standardization Allergen Engineering Research Center, Shenzhen University, Shenzhen, Guangdong 518055, P.R. China; [5]Emergency Department, The Second Affiliated Hospital, School of Medicine, The Chinese University of Hong Kong, Longgang District People's Hospital of Shenzhen, Shenzhen, Guangdong 518100, P.R. China

Received June 30, 2025; Accepted October 14, 2025

DOI: 10.3892/mmr.2025.13787

Abstract. Recurrence and metastasis are the leading causes of poor prognosis and death in lung cancer, and the mechanism of cancer metastasis has not yet been fully elucidated. As a gut-specific homeobox (HOX) transcription factor, intestine-specific HOX (ISX) is a proto-oncogene induced by the inflammatory factor IL-6. Notably, ISX overexpression can induce the epithelial-mesenchymal transition (EMT) response, and promotes tumor cell migration and invasion. In the present study, a lung cancer cell model with overexpression of ISX was established by infecting lung cancer cells with lentivirus. Reverse transcription-quantitative polymerase chain reaction was first used to verify the expression of the EMT-related gene induced by ISX overexpression. Furthermore, transcriptome sequencing and analysis showed that the overexpression of ISX induced significant changes in the gene expression profile of human lung cancer cells. In addition, type I collagen α1 chain (COL1A1), a highly expressed gene in various tumor tissues and cells, was shown to promote tumor cell migration and invasion, possibly by promoting EMT, and was significantly upregulated in human lung cancer cells overexpressing ISX. These results suggested that ISX may promote lung cancer migration and invasion by increasing the expression of COL1A1. In addition, four drugs that are currently used to treat lung cancer were screened. Of these, Iressa® (gefitinib) was revealed to significantly inhibit the viability, migration and invasion of lung cancer cells that stably overexpress ISX by downregulating the expression of COL1A1. In conclusion, these findings may help to prevent tumor metastasis and spread, and the potential molecular mechanism by which ISX promotes the development and migration of lung cancer was suggested. The current findings provide novel targets, and a scientific basis for the prevention and treatment of lung cancer, which may reduce costs for patients, their families and society.

Correspondence to: Dr Qinmiao Huang, Department of Respiratory Medicine and Allergy, The Third Affiliated Hospital (The Affiliated Luohu Hospital) of Shenzhen University, 47 Youyi Road, Luohu, Shenzhen, Guangdong 518000, P.R. China
E-mail: hqmwwb@163.com

Dr Jingyan Liu, Emergency Department, The Second Affiliated Hospital, School of Medicine, The Chinese University of Hong Kong, Longgang District People's Hospital of Shenzhen, 53 Ai Xin Road, Longgang, Shenzhen, Guangdong 518100, P.R. China
E-mail: liujy2597@126.com

*Contributed equally

Key words: intestine-specific homeobox, type I collagen α1 chain, lung cancer, migration, invasion

Introduction

Lung cancer is the leading cause of cancer morbidity and mortality. According to the results of a study published in 2024 based on global cancer statistics, there were ~2.5 million new cases of lung cancer and >1.8 million associated deaths in 2022, accounting for ~1/8 (12.4%) of all cancer diagnoses and 1/5 (18.7%) of all cancer-related deaths worldwide (1). The incidence and mortality rates of lung cancer vary among different countries and regions, with higher rates observed among men and in countries with a higher human development index. With the growth in human development index, it is expected that lung cancer incidence and mortality will markedly increase in the coming decades (2).

Recurrence and metastasis are the leading causes of poor prognosis and death in lung cancer. Although a number of studies have explored cancer metastasis, the underlying mechanism of action has not yet been fully elucidated (3). Homeobox (HOX) genes are a superfamily of transcription factors containing homeodomains that control cell

proliferation, differentiation and morphological changes during the early stages of embryonic development (4). The dysregulation of HOX genes enhances cell survival and proliferation, and inhibits cell differentiation. Previous studies have revealed that numerous HOX genes are abnormally expressed in various types of human tumor, such as bladder, breast, lung, liver, colorectal, prostate and ovarian cancer (5-8).

As a recently identified HOX transcription factor, the intestine-specific HOX (ISX) gene is specifically expressed in the adult and fetal intestine (9). ISX is a proto-oncogene that is upregulated in hepatocellular carcinoma (HCC) through the induction of proinflammatory cellular factors. Notably, it can bind directly to the cyclin D1 promoter in the nucleus, thereby regulating the proliferation of tumor cells, and it is also an important activator of proliferation and tumorigenesis *in vivo* (10). In addition, ISX is highly expressed in lung cancer cells and patient tissue; its upregulation can accelerate the migration and invasion of lung cancer cells and higher levels of ISX expression in lung cancer tissues indicate more obvious lymph node metastasis (11). Previous studies have reported that ISX expression can induce an epithelial-mesenchymal transition (EMT) response, promoting tumor cell migration and invasiveness (10,11); however, the underlying mechanisms are not yet fully understood. Therefore, it is important to explore the potential mechanism underlying the regulation of metastasis for the prevention and treatment of lung cancer.

The present study aimed to establish a cell model with enhanced migration and invasion properties by lentivirus-mediated overexpression of the ISX oncogene, which was assessed using cellular and molecular biology technologies. The current study examined how ISX induces and participates in the development of the tumor microenvironment, thereby promoting tumor cell migration and invasion and progression. Transcriptomics analysis was employed to further investigate potential ISX-promoted lung cancer migration biomarkers and molecular mechanisms. Furthermore, the therapeutic efficacy of currently available lung cancer drugs was verified in a cell model with stable overexpression of ISX. The study aimed to identify novel options to treat lung cancer, and to provide a scientific basis for its prevention and treatment, which may reduce the cost to patients, their families and society.

Materials and methods

Cell culture. A549 human non-small cell lung cancer (NSCLC) cells (cat. no. ZQ003) were purchased from Shanghai Zhongqiao Xinzhou Biotechnology Co., Ltd. The cells were cultured in Dulbecco's Modified Eagle Medium supplemented with 10% fetal bovine serum (FBS) and 1% penicillin/streptomycin (100 U/ml) (all from Gibco; Thermo Fisher Scientific, Inc.) at 37˚C and 5% CO_2. The medium was changed every 3 days. When the cells reached the logarithmic growth phase, they were passaged and used for subsequent experiments.

Lentiviral infection. GFP-labeled lentiviral vectors overexpressing ISX [Lv-ISX (Ubc-NM_001303508.2-3FLAG-CBh-gcGFP-IRES-puromycin; Gene: ISX Human, gene ID: 91464; transcribed transcript: NM_001303508.2)] and a negative control lentiviral vector (Ubc-MCS-3FLAG-CBh-gcGFP-IRES-puromycin) were obtained from Shanghai GeneChem Co., Ltd. A549 cells in the logarithmic growth phase were harvested, trypsinized and counted. The cell density was adjusted to $2x10^5$ cells/well for inoculation into 6-well plates, 2 ml complete medium was added, and the plates were incubated at 37˚C and 5% CO_2 overnight to allow the cells to attach to the wall and reach 30-50% confluence. First, a preliminary experiment involving viruses with different multiplicity of infection (MOI) gradients was conducted to determine the minimum effective infection dose (MOI, 10). Based on the pre-experiment result, 1 ml medium containing the virus at an MOI of 10 was added to each well. After 24 h of incubation, the medium was removed and fresh medium was added. The transfection efficiency was observed under a fluorescence microscope after 48 h. If the proportion of GFP-labeled cells reaches >80%, the cells were harvested for further validation by reverse transcription-quantitative polymerase chain reaction (RT-qPCR) and western blotting. The validated cells were either screened in a cell culture medium supplemented with 1 μg/ml puromycin for continued culture or cryopreserved in liquid nitrogen for use in subsequent experiments.

Western blot analysis. Total protein was extracted from the cells using RIPA buffer (cat. no. G2002; Wuhan Servicebio Technology Co., Ltd.) according to the manufacturer's instructions, and the protein concentration was measured using a BCA assay. Protein samples were subjected to SDS-PAGE on 12% gels at a loading volume of 10 μl/well (total protein, 30 μg) and then transferred to PVDF membranes. The membranes were incubated for 1 h at room temperature with 5% non-fat milk/TBS-0.1% Tween-20 (TBST) and were then washed five times with TBST. Subsequently, the membranes were incubated overnight at 4˚C with anti-ISX (1:100; cat. No. sc-398934; Santa Cruz Biotechnology, Inc.) and anti-β-actin (1:500; cat. No. sc-58673; Santa Cruz Biotechnology, Inc.) antibodies, followed by incubation with a horseradish peroxidase-coupled secondary antibody (1:2,000; cat. No. 7076; Cell Signaling Technology, Inc.) for 1 h at room temperature. Finally, the membranes were incubated with ECL solution (cat. no. G2014; Wuhan Servicebio Technology Co., Ltd.), and the images were exposed and developed. Protein expression was analyzed semi-quantitatively using ImageJ2 (Fiji; National Institutes of Health).

RT-qPCR analysis. RT-qPCR detection was performed using the RNA extracted from A549 cells with or without ISX overexpression, as well as from A549 cells overexpressing ISX treated with 25 μg/ml gefitinib (Iressa®; cat. no. HY-50895; MedChemExpress) for 48 h in a cell incubator at 37˚C. Total RNA was extracted from these cells using the EZ-10 DNA-free RNA Mini-Preps Kit (Sangon Biotech Co., Ltd.) according to the manufacturer's instructions. A total of 1 μg RNA was then reverse transcribed into cDNA using a PrimeScript™ RT Kit with gDNA Eraser (Takara Bio, Inc.) according to the manufacturer's protocol. Briefly, total RNA, 5X PrimeScript RT Master Mix (Perfect Real Time) and RNase Free dH_2O were used to form a reaction system, which was incubated at 42˚C for 15 min, followed by incubation at 85˚C for 5 sec. Subsequently, qPCR was performed using TB Green Premix Ex Taq™ II (Takara Bio, Inc.) according to the manufacturer's

protocol. The reaction system included 2 μl cDNA, 1 μl primer, 12.5 μl 2X TB Green Premix Ex Taq II (Tli RNaseH Plus) and 8.5 μl ddH_2O, and the thermocycling conditions used were as follows: 95˚C for 30 sec, followed by 40 cycles at 95˚C for 5 sec and 60˚C for 30 sec. Melt curve analysis was performed at the end of amplification by increasing the temperature from 65 to 95˚C in 0.5˚C increments every 5 sec to confirm the specificity of the amplification products. The primer sequences used were as follows: GAPDH, forward (F) 5'-TGCACCACCAACTGCTTAGC-3', reverse (R) 5'-GGCATGGACTGTGGTCATGAG-3'; ISX, F 5'-CCTGCTCTCTGCAGGGGT-3', R 5'-CTGTCCATATCACTCCTCCTGGC-3'; TWIST, F 5'-GGAGTCCGCAGTCTTACGAG-3', R 5'-TCTGGAGGACCTGGTAGAGG-3'; Slug, F 5'-ACACATTACCTTGTGTTTGCAAGATCT-3', R 5'-TGTCTGCAAATGCTCTGTTGCAGTG-3'; vimentin (VIM), F 5'-GAGAACTTTGCCGTTGAAGC-3', R 5'-GCTTCCTGTAGGTGGCAATC-3'; zinc finger E-box binding HOX 1 (ZEB1), F 5'-GAAAATGAGCAAAACCATGATCCTA-3', R 5'-CAGGTGCCTCAGGAAAAATGA-3'; and E-cadherin, F 5'-AGAACGCATTGCCACATACACTC-3', R 5'-CATTCTGATCGGTTACCGTGATC-3'. The relative expression levels of the genes were examined using the $2^{-\Delta\Delta Cq}$ method with GAPDH as the reference gene (12).

Transcriptome sequencing. Three replicates of A549 cells with lentivirus infection-mediated ISX overexpression and three replicates of A549 cells infected with the negative control lentiviral vector were used for transcriptome sequencing. These six samples were sent to Beijing Novogene Technology Co., Ltd. for transcriptome sequencing and data analysis. Briefly, RNA was extracted using the TRNzol universal reagent; cat. no. 4992730; Tiangen Biotech Co., Ltd.) method, and the total amounts and integrity of extracted RNA were assessed using the RNA Nano 6000 Assay Kit on the Bioanalyzer 2100 system (Agilent Technologies, Inc.). Upon successful detection, library construction was performed using the NEB Next Ultra™ RNA Library Prep Kit (Illumina, Inc.). After the construction of the library, the library was quantified using the Qubit2.0 Fluorometer (Thermo Fisher Scientific, Inc.), then diluted to 1.5 ng/μl, and the insert size of the library was detected using the Agilent 2100 bioanalyzer. RT-qPCR (Touch q-PCR system CFX96; Bio-Rad Laboratories, Inc.) was used to accurately quantify the effective concentration of the library (the loading concentration of the final library was >2 nM) to ensure the quality of the library. RT-qPCR was performed using TB Green Premix Ex Taq™ II (Takara Bio, Inc.), and the thermocycling conditions used were as follows: 95˚C for 30 sec, followed by 40 cycles at 95˚C for 5 sec and 60˚C for 30 sec. Subsequently, the libraries were pooled according to the required effective concentration and target downstream data volume for Illumina sequencing [Illumina NovaSeq X plus; Illumina MiSeq Reagent Kit v3 (cat. no. MS-102-3003); both from Illumina, Inc.], and 150 bp paired-end reads were generated. The image data of the sequenced fragments measured by the high-throughput sequencer were converted into sequence data (reads) by CASAVA base recognition (version 1.6; Illumina, Inc.). The raw data were then filtered by removing reads containing adapters or 'N' (which indicates that base information could not be determined), as well as low-quality reads (reads with Qphred ≤20 bases accounting for >50% of the entire read length). Subsequently, the Q20 (≥90%) and Q30 (≥85%) values, and the GC content (45-55%) were calculated for the clean and filtered data, and it was ensured that all subsequent analyses were of a high quality and based on clean data. The HISAT2 software (v2.0.5; https://daehwankimlab.github.io/hisat2/) was then used to rapidly and accurately align the clean reads with the reference genome to obtain the localization information of the reads on the reference genome. Intergroup differences and intra-group sample replication were further evaluated through Pearson's correlation analysis and principal component analysis.

The Venn diagram was implemented using the VennDiagram R package (version 1.7.3; https://cran.r-project.org/web/packages/VennDiagram) and the gene expression heatmaps were generated using the ggplot2 (version 3.5.1; https://cran.r-project.org/web/packages/ggplot2/index.html)and pheatmap R packages (version 1.0.2; https://cran.r-project.org/package=pheatmap). After quantifying the gene expression levels, differential expression between the two comparison groups was analyzed using DESeq2 software (version 1.20.0; http://packages.renjin.org/package/org.renjin.bioconductor/DESeq2). The Benjamini-Hochberg method was then used to adjust the obtained P-value (Padj) to control the false discovery rate. The threshold for significant differential expression was set to Padj ≤0.05 and |log2 (fold change)|≥1. The names of each differentially expressed gene (DEG) and the word 'cancer' were used as key words when searching Google Scholar (https://scholar.google.com/) to explore the association between these genes and cancer. The retrieved literature, including research articles and review papers, was further screened based on titles and abstracts, and finally confirmed through the content of the documents. The clusterProfiler (version 3.8.1; https://github.com/YuLab-SMU/clusterProfiler) software was then used to perform Gene Ontology (GO) and Kyoto Encyclopedia of Genomes (KEGG) pathway enrichment analyses on the DEGs. A Padj value of <0.05 was considered significant. The STRING database (v11.5; https://string-db.org/) was further used to construct the protein-protein interaction (PPI) network, and the top five central genes were identified using the Degree algorithm in the CytoHubba plugin of Cytoscape software (version 0.1; https://apps.cytoscape.org/).

Cell Counting Kit 8 (CCK8) assay. The active ingredients of the following established lung cancer drugs were purchased from MedChemExpress: Bevacizumab (Avastin®), erlotinib (Tarceva®), cetuximab (Erbitux®) and gefitinib. Initially, their effects on the viability of uninfected A549 cells were assessed. Specifically, A549 cells with or without ISX overexpression in the logarithmic growth phase were inoculated into 96-well plates at a density of 3,000 cells/well and were cultured for 24 h. Cells not overexpressing ISX were then treated with bevacizumab, erlotinib, cetuximab and gefitinib (100 μl) at concentrations of 0, 5, 25, 30, 35, 40, 45 and 50 μg/ml, and were cultured in the incubator for 48 h. In addition, cells overexpressing ISX were treated with gefitinib under the same conditions. After 48 h, 10 μl CCK8 reagent (cat. no. CK04; Dojindo Laboratories, Inc.) was added to each well. Several wells with only the culture medium added and no cells were used as blank controls. After incubation at 37˚C for 2-4 h, the optical density (OD) at 450 nm was measured using an

ultraviolet spectrophotometer. The cell viability was calculated using the following formula: Cell viability (%)=[(experimental group OD-blank group OD)/(control group OD-blank group OD)] x100.

Wound healing assay. Cells overexpressing ISX in the logarithmic growth phase were collected, digested with trypsin into a single-cell suspension and inoculated at a density of $1x10^5$ cells/well into a 6-well culture plate to ensure that the fusion rate of the inoculated cells reached >90% overnight. Subsequently, a sterile pipette tip was used to make a straight scratch on the cell monolayer, followed by a wash with phosphate-buffered saline to remove the exfoliated cells. An initial image of the scratch was captured under a fluorescence microscope and recorded as 0 h. Subsequently, the medium was replaced with low-serum (1% FBS) medium with or without gefitinib. After culturing for a further 48 h, images were captured from the same position as at 0 h to record the closure of the scratches. Images of the scratch area were analyzed using ImageJ software and the scar healing analysis plug-in (MRI_Wound_Healing_Tool; https://www.mri.cnrs.fr/en/data-analysis/software-and-tools/271-mri-tools/409-wound-healing-tool.html) was used to measure cell migration. Migration rate (%)=(48 h scratch area-0 h scratch area)/0 h scratch area x100.

Cell invasion assay. A Transwell invasion assay was conducted using Transwell cell chambers (24-well plates; pore size, 8 μm) that were coated with Matrigel. Briefly, Matrigel was diluted in PBS at a 1:8 ratio under 4˚C conditions (on ice). Subsequently, 50 μl was added evenly to the upper chamber surface of the Transwell chamber and incubated at 37˚C for 4 h to allow the Matrigel to polymerize into a gel film. A549 cells overexpressing ISX in the logarithmic growth phase were assessed. Briefly, after digestion, cells were resuspended in serum-free medium, and 250 μl cells ($8x10^4$/well) were transferred to the upper chamber of the Transwell. Different concentrations of gefitinib diluted in medium containing 10% FBS (0, 25 and 50 μg/ml) were added to the lower chamber. The cells were incubated for 48 h to allow the cells to penetrate the Matrigel and to migrate into the lower chamber. Subsequently, the non-invasive cells were removed from the upper chamber with a cotton swab, and the lower chamber membrane was fixed with 4% paraformaldehyde for 30 min followed by staining with 0.2% crystal violet for 10 min at room temperature. Observations were made and images were captured under a light microscope. Finally, the crystal violet was completely eluted by thoroughly shaking the solution in 3% acetic acid at room temperature for 5 min. The eluate was then used to measure the OD value at 570 nm using a microplate reader.

Statistical analysis. All data are presented as the mean ± SEM (n≥3) of three independent experiments. The results were statistically analyzed using GraphPad Prism 9.0 software (Dotmatics). Statistical differences between the two groups were analyzed using an unpaired Student's t-test. Statistical differences among multiple groups were analyzed using ANOVA followed by Tukey's multiple comparisons post hoc test to identify the groups with significant differences. $P<0.05$ was considered to indicate a statistically significant difference.

Results

Overexpression of the carcinogenic factor ISX promotes the expression of EMT-related genes. To explore the potential role of the oncogene ISX in regulating downstream genes associated with EMT in lung cancer metastasis and its molecular mechanisms, ISX overexpression was induced in A549 lung cancer cells using lentiviral infection and the expression of EMT markers was verified. The MOI and optimal conditions for lentiviral infection of cells were first determined through preliminary experimentation, the results of which are shown in Fig. 1A. Using an MOI of 10 resulted in healthy cells with high fluorescence expression and an infection efficiency of >80%. Subsequently, the mRNA and protein expression levels of ISX were verified by RT-qPCR and western blotting. The results showed that both the mRNA and protein expression levels of ISX were significantly increased after lentiviral infection (Fig. 1B and C). Subsequent experiments were conducted using A549 cells overexpressing ISX. The effects of ISX overexpression on the expression of EMT markers were further validated (Fig. 1D). Consistent with the findings of previous reports (10,11), ISX overexpression significantly increased the expression levels of the EMT markers TWIST, Slug, VIM and ZEB1, while downregulating the expression of the epithelial cell marker E-cadherin.

ISX overexpression significantly alters the gene expression profile of human lung cancer cells. The present study aimed to investigate the mechanisms related to the promotion of tumor cell metastasis and progression by the oncogenic factor ISX, and to discover their possible underlying mechanisms and biomarkers. Briefly, transcriptome sequencing was performed on A549 cells overexpressing ISX via lentiviral infection and on A549 cells infected with the control lentivirus vector (n=3 samples/group). The sequencing data were uploaded to the Sequence Read Archive of the National Center for Biotechnology Information under the accession number PRJNA1282884.

Table SI summarizes the sequencing metrics and quality check results for the raw RNA sequencing reads. After excluding reads containing aptamers, one N base or low quality, 46,016,622, 39,526,880, and 44,502,284 clean reads were obtained in the control groups (Con1, Con2, and Con3), whereas 45,903,940, 44,323,396, and 43,279,598 clean reads were obtained in the ISX overexpression groups (Lv_ISX1, Lv_ISX2, and Lv_ISX3). The sequencing error rate for each library was 0.01%, and >95% of the clean read data had Phred-like quality scores at the Q30 level (error probability of 0.001), indicating high sequencing quality. The total mapping rate of the reference genome ranged between 94.64 and 95.72%, while a smaller percentage (<5%) of the reference genome's multiple loci were mapped (Table SII, Multi map), further verifying the reliability of the sequencing quality. Pearson's correlation analysis and principal component analysis were performed on the two groups of samples to investigate their similarities and differences. The results showed that samples within the same group were highly similar, whereas samples in different groups were dissimilar (Fig. 2A and B). The Venn diagram (Fig. 2C) showed a total of 11,054 genes in both groups. The clustering heatmap further confirmed the reproducibility of

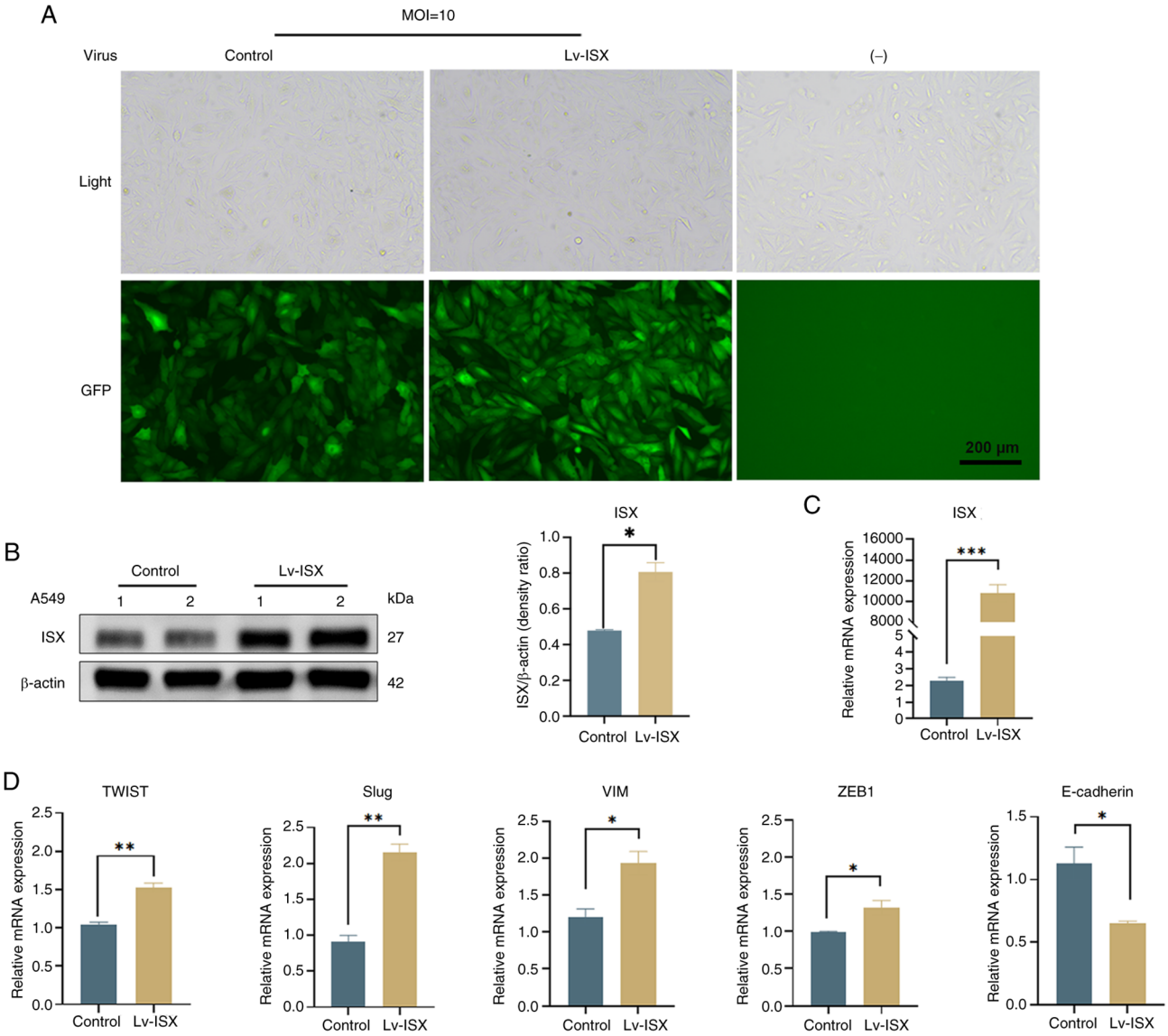

Figure 1. Overexpression of the oncogenic factor ISX promotes the expression of EMT-related genes. (A) ISX overexpression in A549 cells was mediated by Lv infection and observed by GFP fluorescence intensity. Scale bar, 200 μm. (B) ISX protein expression levels were verified by western blot analysis. (C) ISX mRNA expression levels were verified by RT-qPCR detection. (D) Genes related to EMT (TWIST, Slug, VIM and ZEB1) and epithelial cells (E-cadherin) were detected by RT-qPCR. *P<0.05; **P<0.01, ***P<0.001. EMT, epithelial-mesenchymal transition; ISX, intestine-specific homeobox; Lv, lentivirus; MOI, multiplicity of infection; RT-qPCR, reverse transcription-quantitative polymerase chain reaction; VIM, vimentin; ZEB1, zinc finger E-box binding homeobox 1.

the samples, and the global gene expression patterns were revealed to be significantly different between the treatment and control groups (Fig. 2D).

Gene expression analysis was performed on the transcripts to further characterize the DEGs in the ISX overexpression group compared with in the control group. A total of 152 DEGs were identified, 48 of which were upregulated and 104 of which were downregulated (Fig. 3A). The heatmap in Fig. 3B and Table SIII show the upregulated DEGs in the ISX overexpression group. The results of the literature review indicated that most of the DEGs were associated with tumor metastasis. Subsequently, the biological functions and signaling pathways of these genes were comprehensively analyzed by GO functional annotation and KEGG pathway analyses.

KEGG pathway analysis revealed the primary pathways enriched in the upregulated DEGs, including 'proteoglycans in cancer', 'basal cell carcinoma', 'focal adhesion', 'Wnt signaling pathway', 'cytokine-cytokine receptor interaction', 'PI3K-Akt signaling pathway', 'ECM-receptor interaction', 'calcium signaling pathway' and 'Ras signaling pathway' (Fig. 3C). Further functional enrichment analyses revealed that these interacting genes were primarily involved in the following biological processes: 'Connective tissue development', 'cartilage development', 'positive regulation of cell migration', 'regulation of chondrocyte differentiation', 'positive regulation of endothelial cell migration' and 'positive regulation of cell motility'. Enriched cellular components included 'extracellular matrix', 'endoplasmic reticulum lumen' and 'collagen-containing extracellular matrix'. At the molecular function level, these genes were associated with 'collagen binding', 'metalloendopeptidase inhibitor activity', 'cytokine receptor activity', 'immune receptor activity', 'receptor ligand activity' and 'extracellular matrix structural constituent conferring tensile strength' (Fig. 3D). These results

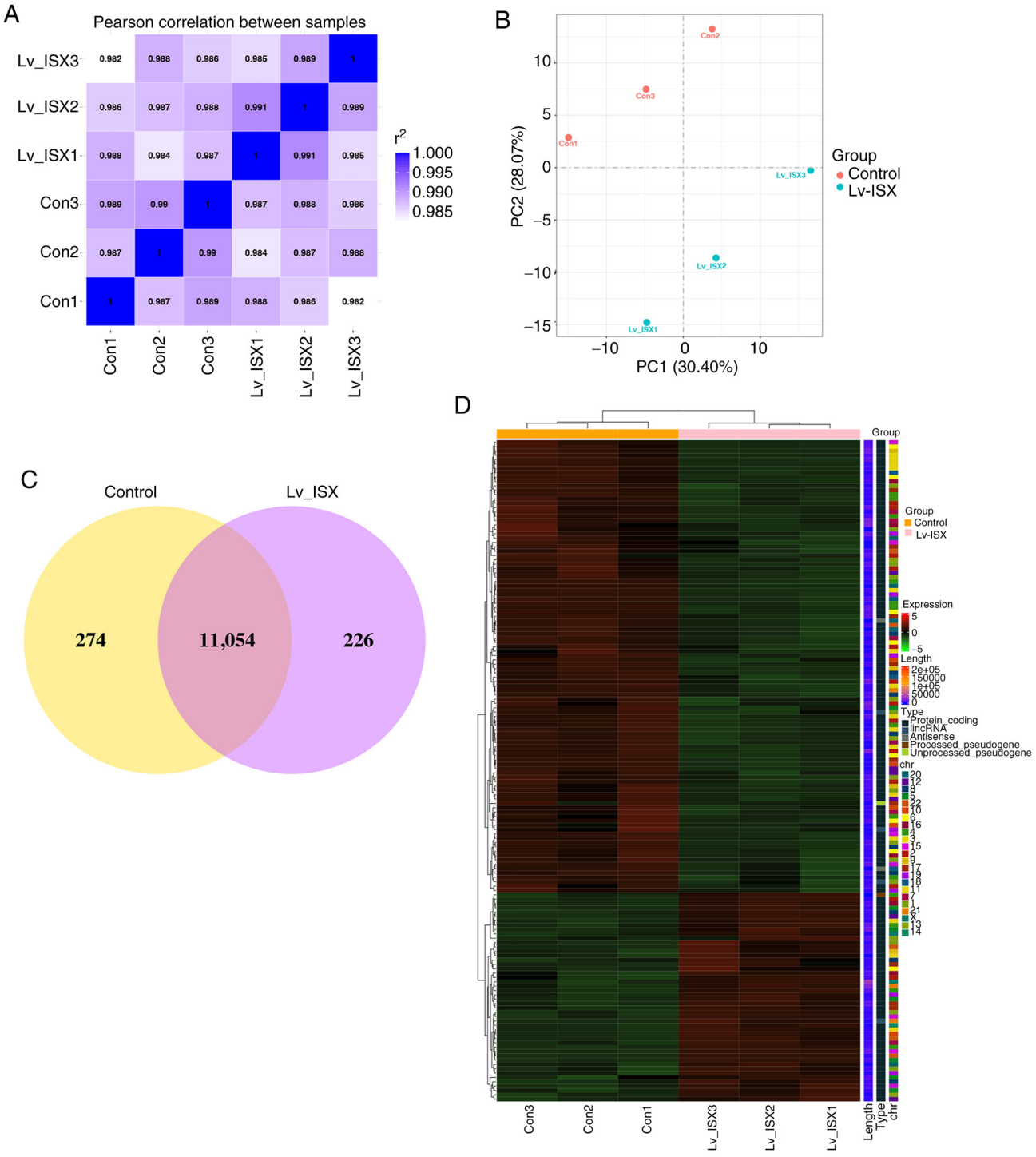

Figure 2. Overexpression of ISX induces significant changes in the gene expression profile of human lung cancer cells. (A) Pearson's correlation analysis comparing the ISX overexpression group with the control group. (B) Principal component analysis comparing the ISX overexpression group with the control group. (C) Venn diagram showing the number of genes shared between the two groups (ISX overexpression and control). (D) Heatmap showing gene expression in the ISX overexpression and control groups. Con, control; ISX, intestine-specific homeobox; Lv, lentivirus

suggested that the overexpression of ISX may contribute to the processes of invasion, migration and cartilage formation in lung cancer cells.

ISX may promote lung cancer migration and invasion by upregulating type I collagen α1 chain (COL1A1). To further investigate the possible mechanism by which ISX overexpression promotes tumor cell migration and invasion, a PPI network was constructed for the upregulated DEGs by using the software program Cytoscape (Fig. 4A). Based on the degree-based topological algorithm, the top five core genes (KDR, COL1A1, SPARC, PDGFB and WNT4), which showed the most significant interactions, were identified using the Cytoscape CytoHubba application (Fig. 4B). Notably, COL1A1 was recognized as one of the hub genes; COL1A1 is a key protein encoding fibrous collagen, the main component

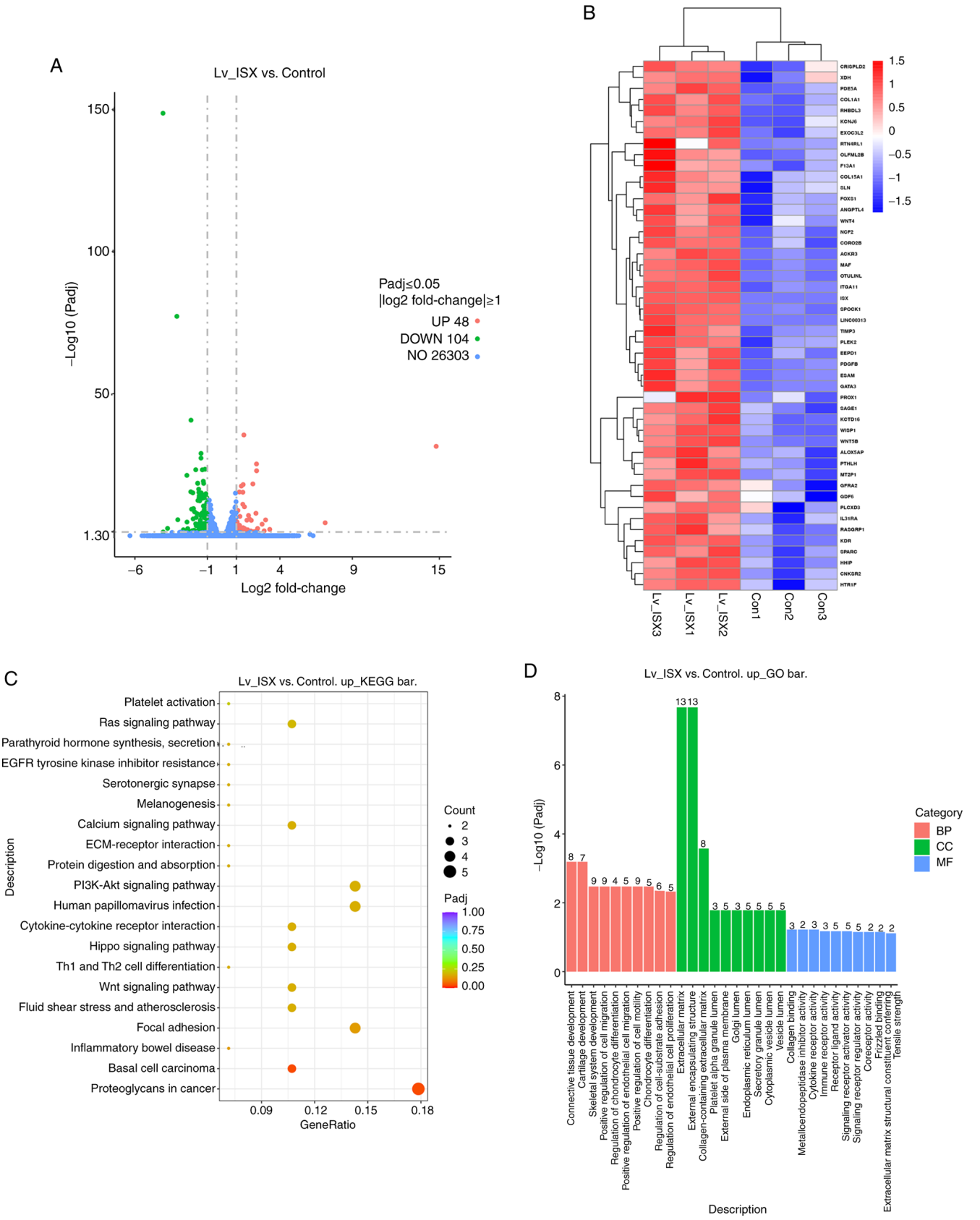

Figure 3. Screening of DEGS in cells with ISX overexpression, and enrichment analyses of biological functions and signaling pathways. (A) Volcano plot showing the number of genes with significant differences in expression levels between the ISX overexpression group and the control group, as well as the specific distribution of DEGs. (B) Heatmap showing the expression of DEGs that were upregulated in the ISX overexpression groups. (C) KEGG analysis showing the top 20 enriched pathways of the DEGs that were upregulated in the ISX overexpression group compared with the control group. Bubble size represents the number of genes, color shade represents Padj, and the enrichment ratio on the y-axis represents the number of genes/total number of genes. (D) GO term enrichment analysis of the DEGs that were upregulated in the ISX overexpression group compared with the control group. The numbers on the columns indicate the number of enriched genes in that category. BP, biological process; CC, cellular component; Con, control; DEG, differentially expressed gene; GO, Gene Ontology; ISX, intestine-specific homeobox; KEGG, Kyoto Encyclopedia of Genes and Genomes; Lv, lentivirus; MF, molecular function.

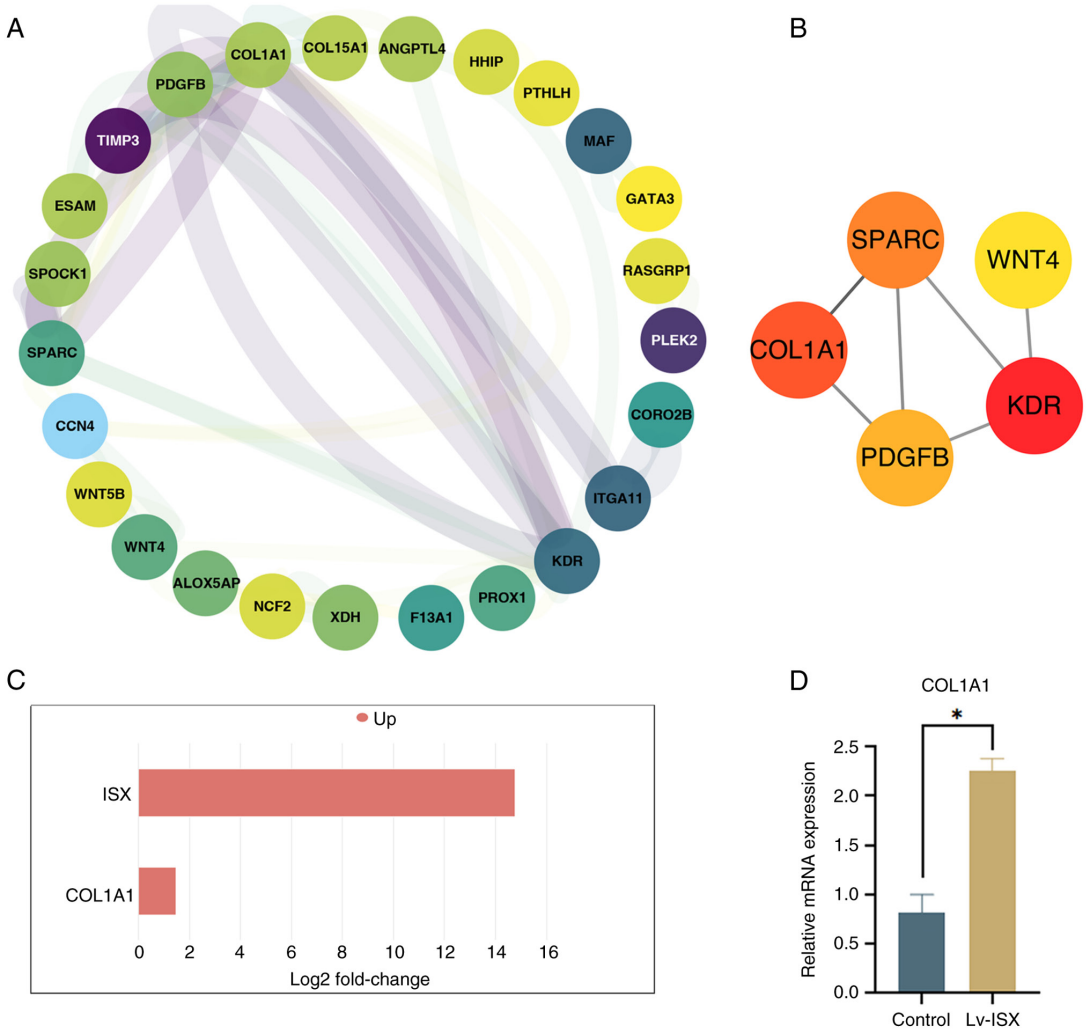

Figure 4. ISX may promote lung cancer migration and invasion by upregulating COL1A1. (A) Upregulated differentially expressed genes in A549 cells with ISX overexpression were selected to construct the PPI network. (B) Five core hub genes were identified in the PPI network. (C) Column chart showing the difference in COL1A1 expression in ISX-overexpressing A549 cells in the transcriptome sequencing results. (D) mRNA expression levels of COL1A1 were verified by reverse transcription-quantitative polymerase chain reaction. *P<0.05. COL1A1, type I collagen α1 chain; ISX, intestine-specific homeobox; Lv, lentivirus; PPI, protein-protein interaction.

of type I collagen, and it server a crucial role in maintaining cell morphology, intercellular connections, tissue structure stability and extracellular matrix (ECM) homeostasis (13). Notably, COL1A1 dysfunction has been shown to be associated with various diseases, including fibrosis, osteogenesis imperfecta and osteoporosis, which are bone diseases caused by COL1A1 deficiency (14). In recent years, multiple reports have shown that COL1A1 is upregulated in various tumor tissues and cells, prompting researchers to pay increasing attention to its role in cancer (15-18).

The transcriptome sequencing results showed that ISX overexpression led to the upregulated expression of COL1A1 (Fig. 4C), which was further verified by RT-qPCR (Fig. 4D). Studies have shown that the abnormal upregulation of COL1A1 in cancer is closely related to regulating tumor cell proliferation, differentiation and migration (15). These findings provide important insights into the specific mechanisms by which COL1A1 may be involved in ISX-induced regulation of tumor migration and invasion. Its potential mechanism awaits further systematic analysis in future research.

Screening of mature tumor-targeting drugs that may be used to treat ISX-induced lung cancer. Metastasis of tumor cells is the primary cause of a poor prognosis for tumors. Notably, the upregulation of ISX may accelerate the migration and invasion of lung cancer cells; therefore, four mature tumor-targeting drugs were used to treat the ISX-induced lung cancer cell model, with the aim of identifying better therapeutic drugs that can resist tumor metastasis. The drugs used in the current study included Iressa (gefitinib), Tarceva (erlotinib) and Avastin (bevacizumab), which are already used to treat lung cancer. Although Erbitux (cetuximab) is approved for treating colorectal cancer and head and neck cancer, as an anti-EGFR monoclonal antibody, it has been extensively studied in combination with chemotherapy for the treatment of advanced NSCLC (19,20). The current study first evaluated the effects of these treatments on the viability of un-infected A549 cells. As shown in Fig. 5A-D, only gefitinib affected A549 cell viability within the tested concentration range (0-50 μg/ml). The concentration range significantly affected A549 cell viability in a dose-dependent

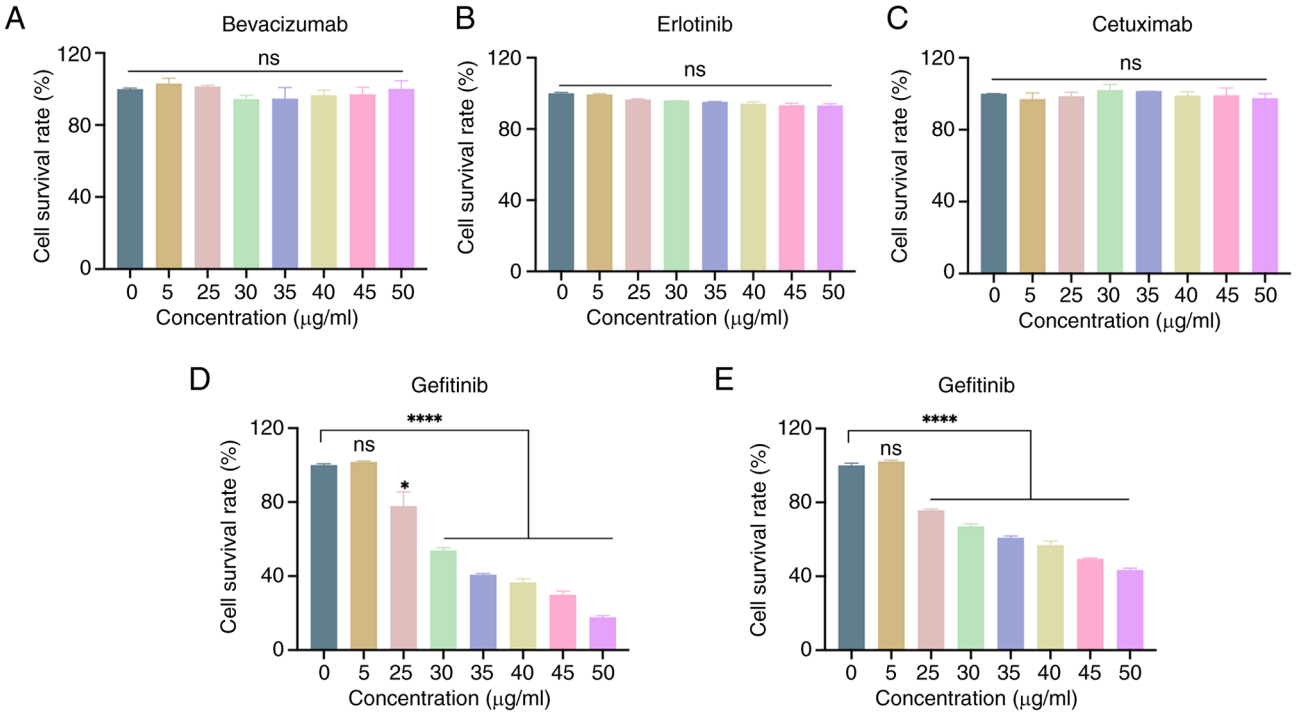

Figure 5. Cell Counting Kit 8 screening to identify mature tumor-targeting drugs that can inhibit the activity of lung cancer cells stably overexpressing ISX. Effects of (A) bevacizumab, the active ingredient of Avastin®, (B) erlotinib, the active ingredient of Tarceva®, (C) cetuximab, the active ingredient of Erbitux® lung cancer drug and (D) gefitinib, the active ingredient of Iressa®, on the survival of lung cancer cells not overexpressing ISX. (E) Effect of gefitinib on the survival of ISX-overexpressing lung cancer cells. *P<0.05; ****P<0.0001; ns, not significant. ISX, intestine-specific homeobox.

manner, starting at 25 μg/ml. Therefore, gefitinib was subsequently used for the treatment of cells stably overexpressing ISX. The results showed that gefitinib was also effective in reducing the viability of A549 cells stably overexpressing ISX at concentrations of ≥25 μg/ml (Fig. 5E), although the reduction in cell viability was not as high as that in non-infected A549 cells.

The effects of gefitinib (the active ingredient of Iressa®) on the migration and invasion characteristics of lung cancer cells with stable overexpression of ISX were then evaluated through wound healing and Transwell assays. The results, as shown in Fig. 6A and B, indicated that gefitinib can significantly inhibit the migration and invasion of ISX-overexpressing A549 lung cancer cells in a concentration-dependent manner. Furthermore, the effects of gefitinib on the expression of ISX, COL1A1 and EMT-related genes were detected by RT-qPCR to preliminarily explore the mechanism of gefitinib in inhibiting the migration and invasion of lung cancer cells stably overexpressing ISX. Although gefitinib had no inhibitory effect on the expression of ISX and EMT-related genes (data not shown), the results showed that it could significantly reduce the upregulation of COL1A1 gene expression caused by ISX (Fig. 6C). These data initially suggested that the mature tumor-targeting drug Iressa® may be a promising therapeutic drug that can resist tumor metastasis, particularly in patients with tumor metastasis caused by high ISX expression. Moreover, the downregulation of COL1A1 gene expression may be considered an important molecular mechanism for its effective resistance to tumor metastasis, which is worthy of in-depth exploration in future studies.

Discussion

As a gut-specific HOX transcription factor, ISX is a proto-oncogene induced by the inflammatory factor IL-6, and previous researchers have identified the effect of ISX on cancer development. In HCC cells, the kynurenine (KYN) pathway promotes oncogenic activity by binding to aryl hydrocarbon receptor (AHR) in an ISX-dependent positive feedback loop. In addition, it has been shown that the ISX-KYN axis upregulates immunosuppressive activity by targeting CD86 and programmed death ligand 1 (PD-L1) expression, thereby suppressing $CD8^{+}$ T-cell proliferative responses. Thus, ISX-KYN-AHR signaling acts together with CD86 and PD-L1 to promote the carcinogenesis and immunosuppression of HCC cells (10). In lung cancer, ISX is highly expressed in lung cancer cells and patient tissues, and its upregulation is positively associated with lung cancer cell migration and invasion. A mechanistic study has shown that the P300/CBP-associated factor (PCAF)-ISX-bromodomain-containing protein 4 (BRD4) axis is an important regulator of lung cancer metastasis and cell plasticity (11). PCAF-mediated acetylation of the transcription factor ISX promotes ISX-BRD4 translocation to the nucleus, which activates EMT genes and induces metastasis (11).

Cancer cell migration is a complex process in which the EMT of cancer cells is the initial step. Although numerous signaling molecules and pathways (such as PI3K, Snail, hypoxia-inducible factor 1α and Smad interacting protein 1) and transcription factors (TWIST1/2, SNAIL1/2, ZEB1/2 and FOXC2) have been proposed to regulate and induce EMT (21), the detailed regulatory mechanisms remain largely unknown.

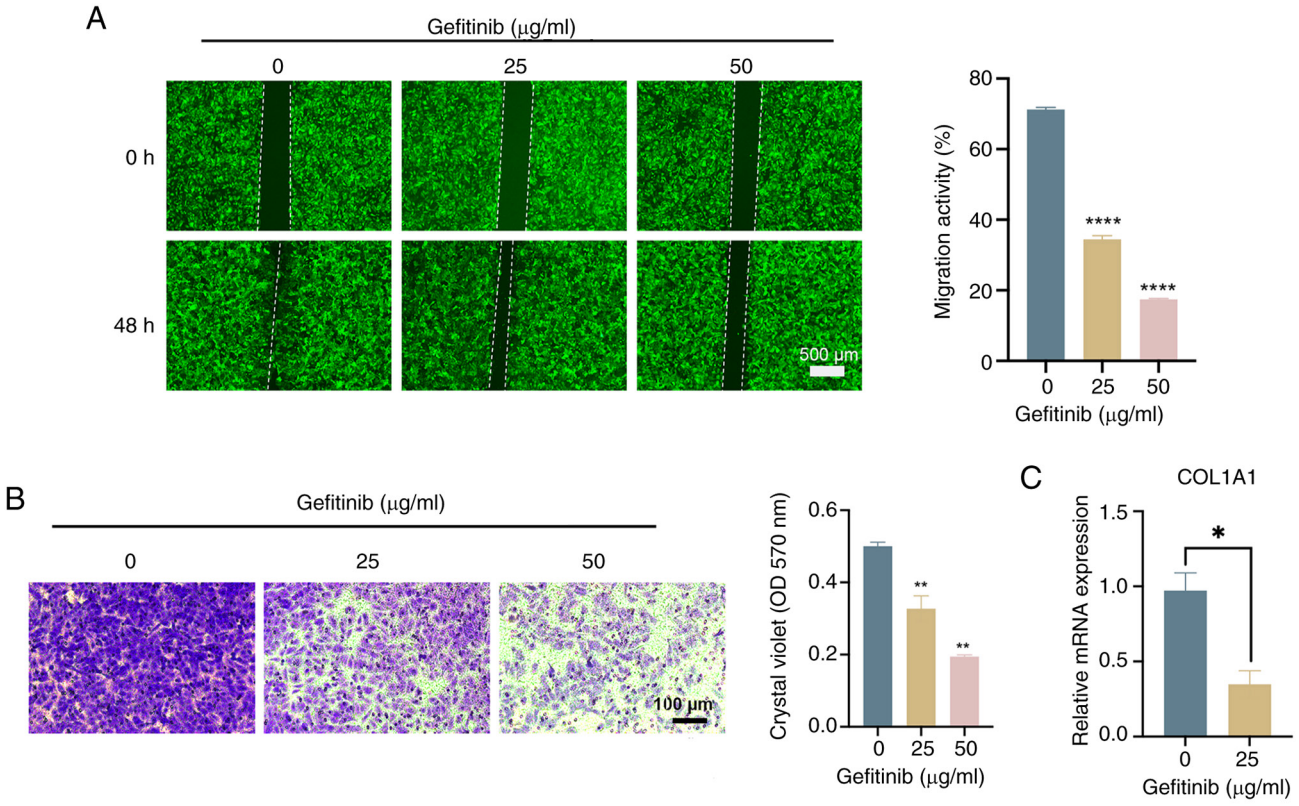

Figure 6. Mature tumor-targeting drug Iressa® (gefitinib) may inhibit the migration and invasion of ISX-overexpressing human lung cancer cells by regulating COL1A1. A549 cells infected with a GFP-labeled ISX overexpression vector were treated with different concentrations of gefitinib (0, 25, 50 μg/ml) for 48 h, and (A) cell migration (wound healing; scale bar, 500 μm, and (B) invasion (Transwell; scale bar, 100 μm) assays were performed. (C) Reverse transcription-quantitative polymerase chain reaction was used to detect the effect of gefitinib (25 μg/ml, 48 h) on the mRNA expression levels of COL1A1 in ISX-overexpressing A549 cells. *P<0.05; **P<0.01; ****P<0.0001. COL1A1, type I collagen α1 chain; ISX, intestine-specific homeobox; OD, optical density.

In the present study, lung cancer cells stably overexpressing ISX were constructed by lentivirus infection, and EMT-related gene expression was detected by RT-qPCR. It was verified that ISX expression induced EMT response, and promoted tumor cell migration and invasion. To further investigate the molecular regulatory mechanisms by which the oncogene ISX enhances tumor cell invasion and migration, transcriptome sequencing and analysis was performed using A549 cells overexpressing ISX. The results revealed that COL1A1 was upregulated in ISX-overexpressing lung cancer cells, which was verified by RT-qPCR. The Cytoscape CytoHubba analysis further identified COL1A1 as a hub gene (one of the top five core genes) in the PPI pathway, indicating that COL1A1 may be involved in the molecular mechanism of ISX-regulated tumor metastasis.

COL1A1 is one of the main components of the ECM, and the dynamic balance of ECM serves a central role in maintaining the tumor microenvironment. Numerous studies have shown that COL1A1 is upregulated in numerous types of cancers and that it can affect various signaling pathways related to those types of cancer, including gastric cancer, lung adenocarcinoma, ovarian cancer, colorectal cancer, breast cancer and thyroid cancer (15,16,22-26). In HCC, knocking down COL1A1 markedly inhibits cell invasion and migration, and downregulates VIM, a protein that promotes the EMT phenotype, thus suggesting that COL1A1 may promote tumor cell migration and invasion by promoting EMT (27). A multi-omics analysis previously identified COL1A1 as a key gene for lung adenocarcinoma development and progression (28). Subsequently, the clinical importance of COL1A1 expression in lung cancer samples and its association with clinical prognosis were determined by detecting the expression levels of COL1A1 in lung cancer samples. The results demonstrated that the mRNA levels and gene amplification of COL1A1 in lung cancer tissues are higher than those in normal lung tissues. Furthermore, COL1A1 was shown to be highly expressed in lung cancer tissues and serum, and high expression of COL1A1 was revealed to be associated with poor progression-free survival and chemotherapy resistance in patients with lung cancer. Therefore, COL1A1 may be used as a novel diagnostic, prognostic and chemoresistance biomarker for human lung cancer (29). Taken together, these findings suggested that ISX may induce EMT by upregulating COL1A1 and could alter the tumor microenvironment, thereby promoting tumor migration and more aggressive lung cancer behavior. This represents a novel mechanism discovered through transcriptome sequencing in the current study. However, only A549 cells were used in subsequent experiments. Further validation through clinical trials is required to determine the specific type of lung cancer associated with this mechanism; this will be a key area assessed in our future research.

Notably, the PI3K/AKT signaling pathway was enriched in the upregulated DEGs of the ISX-overexpressing lung cancer cells. It has been shown that knockdown of COL1A1

can inhibit the progression of gastric cancer by regulating the PI3K/AKT signaling pathway (22). In addition, an association between COL1A1 and the PI3K/Akt signaling pathway has been detected in ovarian cancer. This suggests that COL1A1 may regulate the proliferation, anti-apoptotic ability and migratory potential of ovarian cancer cells via the PI3K/Akt signaling pathway (16). Therefore, the PI3K/AKT signaling pathway may also be involved in the mechanism by which ISX regulates COL1A1 expression in lung cancer. Although studies have shown that the PI3K/AKT pathway serves an important role in tumors (30), to the best of our knowledge, the specific relationship between ISX and COL1A1 and this pathway in lung cancer has not yet been reported. Future studies should further explore the molecular mechanism of ISX regulating lung cancer progression through COL1A1 and PI3K/AKT signaling pathways.

In conclusion, the present study demonstrated that the expression levels of COL1A1 were increased in lung cancer cells overexpressing ISX, and indicated that the PI3K/AKT signaling pathway may be involved in ISX-regulated COL1A1 expression, promoting tumor migration and invasion. In addition, four currently established drugs for lung cancer treatment were screened. Among them, Iressa (gefitinib) significantly inhibited the viability, migration and invasion of lung cancer cells stably overexpressing ISX. The expression of COL1A1 was also significantly down-regulated after gefitinib treatment, indicating that gefitinib may be a promising cancer drug for the treatment of tumor metastasis by inhibiting the upregulation of COL1A1 expression caused by ISX overexpression. The present findings revealed a novel molecular mechanism by which ISX may promote the progression and metastasis of lung cancer. This discovery provides new theoretical insights into the etiology and progression of cancer, offering novel strategies for its prevention and treatment. The aim of these approaches is to alleviate the suffering of patients with lung cancer and to reduce the societal burden associated with the disease.

Acknowledgements

Not applicable.

Funding

The present study was supported by grants from the National Natural Science Foundation (grant nos. 82341060, 82204883 and 82073950), the Science and Technology Planning Project of Guangdong Province (grant nos. 2023A1515012245 and 2022B1515120055), the Science and Technology Program of Shenzhen (grant nos. JCYJ20250604191406009, JCYJ20210324134209026, JCYJ20220531102217038, JCYJ20210324112414038 and JCYJ20220818102005011), the Shenzhen Medical Research Fund (grant no. A2403062), the Special Fund for Economic and Technological Development of Longgang District, Shenzhen Medical Health Technology Project (grant no. LGWJ2021-046), the Science and Technology Planning Project of Nanshan District (grant no. NS2024026) and the State Key Laboratory of Respiratory Disease (grant no. SKLRD-Z-202216).

Availability of data and materials

The data generated in the present study may be requested from the corresponding author. The sequencing data generated in the present study may be found in the National Center for Biotechnology Information Sequence Read Archive database under accession number PRJNA1282884 or at the following URL: https://www.ncbi.nlm.nih.gov/sra/PRJNA1282884.

Authors' contributions

YM, XX, JL and QH conceived and designed the experiments. YM, YC and YL performed the experiments. YH, MG and LT analyzed and interpreted the data. YM and XX wrote the manuscript. XX, and QH revised the manuscript. YM, YL and XX confirm the authenticity of all the raw data. All authors read and approved the final manuscript.

Ethics approval and consent to participate

Not applicable.

Patient consent for publication

Not applicable.

Competing interests

The authors declare that they have no competing interests.

References

1. Bray F, Laversanne M, Sung H, Ferlay J, Siegel RL, Soerjomataram I and Jemal A: Global cancer statistics 2022: GLOBOCAN estimates of incidence and mortality worldwide for 36 cancers in 185 countries. CA Cancer J Clin 74: 229-263, 2024.
2. Cao W, Qin K, Li F and Chen W: Socioeconomic inequalities in cancer incidence and mortality: An analysis of GLOBOCAN 2022. Chin Med J (Engl) 137: 1407-1413, 2024.
3. Fares J, Fares MY, Khachfe HH, Salhab HA and Fares Y: Molecular principles of metastasis: A hallmark of cancer revisited. Signal Transduct Target Ther 5: 28, 2020.
4. Steens J and Klein D: HOX genes in stem cells: Maintaining cellular identity and regulation of differentiation. Front Cell Dev Biol 10: 1002909, 2022.
5. Chin FW, Chan SC and Veerakumarasivam A: Homeobox gene expression dysregulation as potential diagnostic and prognostic biomarkers in bladder cancer. Diagnostics (Basel) 13: 2641, 2023.
6. Feng Y, Zhang T, Wang Y, Xie M, Ji X, Luo X, Huang W and Xia L: Homeobox genes in cancers: From carcinogenesis to recent therapeutic intervention. Front Oncol 11: 770428, 2021.
7. Yadav C, Yadav R, Nanda S, Ranga S, Ahuja P and Tanwar M: Role of HOX genes in cancer progression and their therapeutical aspects. Gene 919: 148501, 2024.
8. Jasim SA, Farhan SH, Ahmad I, Hjazi A, Kumar A, Jawad MA, Pramanik A, Altalbawy FMA, Alsaadi SB and Abosaoda MK: Role of homeobox genes in cancer: Immune system interactions, long non-coding RNAs, and tumor progression. Mol Biol Rep 51: 964, 2024.
9. Gill HK, Yin S, Nerurkar NL, Lawlor JC, Lee C, Huycke TR, Mahadevan L and Tabin CJ: Hox gene activity directs physical forces to differentially shape chick small and large intestinal epithelia. Dev Cell 59: 2834-2849.e9, 2024.
10. Wang LT, Chiou SS, Chai CY, His E, Yokoyama KK, Wang SN, Huang SK and Hsu SH: Intestine-specific homeobox gene ISX integrates IL6 signaling, tryptophan catabolism, and immune suppression. Cancer Res 77: 4065-4077, 2017.

11. Wang LT, Liu KY, Jeng WY, Chiang CM, Chai CY, Chiou SS, Huang MS, Yokoyama KK, Wang SN, Huang SK and Hsu SH: PCAF-mediated acetylation of ISX recruits BRD4 to promote epithelial-mesenchymal transition. EMBO Rep 21: e48795, 2020.
12. Livak KJ and Schmittgen TD: Analysis of relative gene expression data using real-time quantitative PCR and the 2(-Delta Delta C(T)) method. Methods 25: 402-408, 2001.
13. Devos H, Zoidakis J, Roubelakis MG, Latosinska A and Vlahou A: Reviewing the regulators of COL1A1. Int J Mol Sci 24: 10004, 2023.
14. Selvaraj V, Sekaran S, Dhanasekaran A and Warrier S: Type 1 collagen: Synthesis, structure and key functions in bone mineralization. Differentiation 136: 100757, 2024.
15. Li X, Sun X, Kan C, Chen B, Qu N, Hou N, Liu Y and Han F: COL1A1: A novel oncogenic gene and therapeutic target in malignancies. Pathol Res Pract 236: 154013, 2022.
16. Xiao X, Long F, Yu S, Wu W, Nie D, Ren X, Li W, Wang X, Yu L, Wang P and Wang G: Col1A1 as a new decoder of clinical features and immune microenvironment in ovarian cancer. Front Immunol 15: 1496090, 2025.
17. Liu Y, Xue J, Zhong M, Wang Z, Li J and Zhu Y: Prognostic prediction, immune microenvironment, and drug resistance value of collagen type I alpha 1 chain: From gastrointestinal cancers to pan-cancer analysis. Front Mol Biosci 8: 692120, 2021.
18. Zhang C, Liu S, Wang X, Liu H, Zhou X and Liu H: COL1A1 Is a potential prognostic biomarker and correlated with immune infiltration in mesothelioma. Biomed Res Int 2021: 5320941, 2021.
19. Ribeiro Gomes J and Cruz MRS: Combination of afatinib with cetuximab in patients with EGFR-mutant non-small-cell lung cancer resistant to EGFR inhibitors. Onco Targets Ther 8: 1137-1142, 2015.
20. Della Corte CM, Fasano M, Ciaramella V, Cimmino F, Cardnell R, Gay CM, Ramkumar K, Diao L, Di Liello R, Viscardi G, *et al*: Anti-tumor activity of cetuximab plus avelumab in non-small cell lung cancer patients involves innate immunity activation: Findings from the CAVE-Lung trial. J Exp Clin Cancer Res 41: 109, 2022.
21. Chanvorachote P, Petsri K and Thongsom S: Epithelial to mesenchymal transition in lung cancer: Potential EMT-targeting natural product-derived compounds. Anticancer Res 42: 4237-4246, 2022.
22. Ding Y, Zhang M, Hu S, Zhang C, Zhou Y, Han M, Li J, Li F, Ni H, Fang S and Chen Q: MiRNA-766-3p inhibits gastric cancer via targeting COL1A1 and regulating PI3K/AKT signaling pathway. J Cancer 15: 990-998, 2024.
23. Wang Y, Mei X, Song W, Wang C and Qiu X: LncRNA LINC00511 promotes COL1A1-mediated proliferation and metastasis by sponging miR-126-5p/miR-218-5p in lung adenocarcinoma. BMC Pulm Med 22: 272, 2022.
24. Li Y, Sun R, Zhao X and Sun B: RUNX2 promotes malignant progression in gastric cancer by regulating COL1A1. Cancer Biomark 31: 227-238, 2021.
25. Zhang Z, Wang Y, Zhang J, Zhong J and Yang R: COL1A1 promotes metastasis in colorectal cancer by regulating the WNT/PCP pathway. Mol Med Rep 17: 5037-5042, 2018.
26. Huang C, Yang X, Han L, Fan Z, Liu B, Zhang C and Lu T: The prognostic potential of alpha-1 type I collagen expression in papillary thyroid cancer. Biochem Biophys Res Commun 515: 125-132, 2019.
27. Ma HP, Chang HL, Bamodu OA, Yadav VK, Huang TY, Wu ATH, Yeh CT, Tsai SH and Lee WH: Collagen 1A1 (COL1A1) is a reliable biomarker and putative therapeutic target for hepatocellular carcinogenesis and metastasis. Cancers (Basel) 11: 786, 2019.
28. Yang Z, Liu B, Lin T, Zhang Y, Zhang L and Wang M: Multiomics analysis on DNA methylation and the expression of both messenger RNA and microRNA in lung adenocarcinoma. J Cell Physiol 234: 7579-7586, 2019.
29. Hou L, Lin T, Wang Y, Liu B and Wang M: Collagen type 1 alpha 1 chain is a novel predictive biomarker of poor progression-free survival and chemoresistance in metastatic lung cancer. J Cancer 12: 5723-5731, 2021.
30. Noorolyai S, Shajari N, Baghbani E, Sadreddini S and Baradaran B: The relation between PI3K/AKT signalling pathway and cancer. Gene 698: 120-128, 2019.

Copyright © 2025 Ma et al. This work is licensed under a Creative Commons Attribution-NonCommercial-NoDerivatives 4.0 International (CC BY-NC-ND 4.0) License.